

Femtosecond Studies of Charge-Transfer Mediated Proton Transfer in 2-Butylamino-6-methyl-4-nitropyridine *N*-Oxide

Benedek Poór,^{†,‡} Natalia Michniewicz,^{†,||} Mihály Kállay,[‡] Wybren Jan Buma,^{*,†} Miklós Kubinyi,^{*,‡,§} Anna Szemik-Hojniak,^{||} Irena Deperasińska,[⊥] Aniela Puszko,[#] and Hong Zhang^{*,†}

Van't Hoff Institute for Molecular Sciences, University of Amsterdam, Nieuwe Achtergracht 166, 1018 WV Amsterdam, The Netherlands, Department of Physical Chemistry, Budapest University of Technology and Economics, P.O.B. 91, 1521 Budapest, Hungary, Chemical Research Center, Hungarian Academy of Sciences, P.O.B. 17, 1525 Budapest, Hungary, Faculty of Chemistry, University of Wrocław, PL-50383 Wrocław, Poland, Institute of Physics, Polish Academy of Sciences, Al. Lotników 32/46, 02-668 Warsaw, Poland, and Institute of Chemical and Food Technology, University of Economics, Pl-53 345 Wrocław, Poland

Received: March 7, 2006; In Final Form: April 7, 2006

We have unraveled the effects of an amino substituent in the ortho position on the excited-state dynamics of 4-nitropyridine *N*-oxide by studying the picosecond fluorescence kinetics and femtosecond transient absorption of a newly synthesized compound, 2-butylamino-6-methyl-4-nitropyridine *N*-oxide, and by quantum chemical calculations. Similar to the parent compound, the S_1 state of the target molecule has significant charge-transfer character and shows a large (~ 8000 cm⁻¹) static Stokes shift in acetonitrile. Analysis of the experimental and the theoretical results leads, however, to a new scenario in which this intramolecular charge transfer triggers in polar, aprotic solvents an ultrafast (around 100 fs) intramolecular proton transfer between the amino and the N–O group. The electronically excited N–OH tautomer is subsequently subject to solvent relaxation and decays with a lifetime of ~ 150 ps to the ground state.

I. Introduction

Heterocyclic *N*-oxides increasingly attract attention due to their wide range of applications in biochemistry and photochemistry. They are used as synthetic intermediates, protecting groups, auxiliary agents, oxidants, ligands in metal complexes, and catalysts.^{1,2} One of the primary examples is 4-nitropyridine *N*-oxide and its derivatives that were reported to have an exceptionally high bioactivity.^{3,4} In these systems, it was concluded that the change of the electronic system induced by the nitro group into the 4-position plays a decisive role; for example, the nitro group was found to be essential for developing the antifungal efficiency of a number of substituted 4-nitropyridine *N*-oxides.⁵

Apart from their chemical properties, many of these compounds are also of immediate interest because of their nonlinear optical properties⁶ that are directly related to the asymmetric π electron system. When assisted by intramolecular charge-transfer (ICT) processes, these nonlinear properties can be amplified by a further 2–3 orders of magnitude as compared to aliphatic molecules of the same size.^{7,8} The ICT character of 4-nitropyridine *N*-oxide makes it a proper solvatochromic indicator.⁹ In trying to optimize this feature, one would in general consider primarily the push–pull property of the *N*-oxide and the effect

of the functional groups on the CT process. An aspect that is less often considered, however, are intramolecular dynamic processes that may interfere destructively with the basic charge-transfer mechanism from the *N*-oxide group to the nitro group. Despite the fact that the electronic and structural properties of 4-nitropyridine *N*-oxide are relatively well documented, the photophysical properties of its derivatives, which are strongly sensitive to substituent and substituting position,¹⁰ are far less understood.

Here, we report on the intramolecular photoinduced processes and their influence on the electronic and optical properties of a newly synthesized nitropyridine *N*-oxide derivative, 2-butylamino-6-methyl-4-nitropyridine *N*-oxide (2B6M) (Figure 1). This molecule is an excellent model compound for studying the effects of the interaction between an *N*-oxide group and an amino substituent in the ortho position, which may result in proton transfer in the ground and/or excited electronic states.

The mechanism of excited-state proton transfer (ESPT) has been and still is the subject of extensive research, as evidenced by the rapid growth of the number of publications (see ref 11 and references therein). For intermolecular proton transfer, the following fundamental steps were proposed: electronic excitation induces a charge redistribution that triggers a change of the hydrogen-bond strengths, and this change induces the proton transfer itself. The first step in this proton transfer mechanism is therefore strongly influenced by the solvent polarity. For excited-state intramolecular proton transfer (ESIPT), this picture has been studied with ultrafast spectroscopy.^{12–25}

In the present study, we have performed femtosecond time-resolved spectroscopy and quantum chemical calculations on 2B6M and have found that in a polar, aprotic solvent an

* Corresponding author. Phone: +31-20-5256976. E-mail: hong@science.uva.nl.

[†] University of Amsterdam.

[‡] Budapest University of Technology and Economics.

[§] Hungarian Academy of Sciences.

^{||} University of Wrocław.

[⊥] Polish Academy of Sciences.

[#] University of Economics.

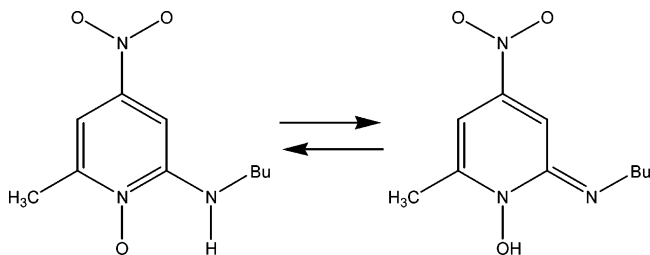


Figure 1. Chemical structures of 2-butylamino-6-methyl-4-nitropyridine *N*-oxide (2B6M) (left) and of its *N*-O-H tautomer (right).

extremely fast (around 100 fs) ESIPT process occurs upon photoexcitation, followed by a solvent reorganization process that is for the most part responsible for the large Stokes shift. This clearly differs from 4-nitropyridine *N*-oxide and some of its derivatives, in which ICT in the electronically excited state is widely accepted to be responsible for the Stokes shift in polar solvents.^{7,8}

II. Experimental and Computational Methods

2-Butylamino-6-methyl-4-nitropyridine *N*-oxide was obtained by mixing of equimolar amounts (0.01 M) of 2-chloro-4-nitro-6-methylpyridine *N*-oxide and butylamine in 40 cm³ volume of ethanol. The mixture was refluxed for 4 h, ethanol was evaporated, water was added, and the precipitate was filtered off. Recrystallization from petroleum ether gave a 76% yield of 2B6M (mp 98 °C). Its purity was checked by GC/MS. Elemental analysis gives rise to the following composition (calculated numbers in parentheses) (%): C, 55.01 (54.77); H, 6.88 (6.90); N, 16.57 (16.43). Cyclohexane was used as purchased (Uvasol, spectroscopic grade). In the case of acetonitrile, experiments were initially performed as well using the solvent as purchased (Uvasol, spectroscopic grade). Experiments using acetonitrile as a solvent gave, however, rise to the suspicion that water dissolved in acetonitrile might dominantly influence the results. Additional experiments were therefore performed with acetonitrile that has been dried over type 3A molecular sieves prior to use. Both experiments gave rise to the same results and therefore exclude a possible role of water.

Steady-state electronic absorption and fluorescence spectra were recorded by a Hewlett-Packard 8453 diode array single-beam spectrophotometer and a Spex Fluorolog 1681 spectrometer, respectively. Emission spectra were corrected for source intensity and detector response by standard correction curves. Fluorescence lifetimes were measured using a time-correlated single photon counting (TC-SPC) setup²⁶ with a time response of ~16 ps (fwhm).

The ultrafast dynamics following femtosecond pulse excitation was studied by femtosecond transient absorption.²⁷ Briefly, a ~100 fs laser pulse train with ~1 mJ/pulse at a repetition rate of 1 kHz, generated using an amplified Ti:Sapphire laser system (Spectra-Physics Hurricane), was split into two beams. One beam pumped an OPA to produce UV pulses that excited the sample; the other (~150 μJ/pulse) was used to generate a white light continuum in the range from 350 to 900 nm to probe the photoinduced changes in absorption. The angle between pump and probe beam was typically 7–10°. Measurements were performed such that the pump beam irradiated a larger area of the sample as compared to the probe beam to guarantee a homogeneous optical density throughout the probing area. The instrument response function is about 200 fs. Components and collection protocol for the transient absorption are driven by homemade software in a Labview environment. These experiments as well as the picosecond TC-SPC experiments were

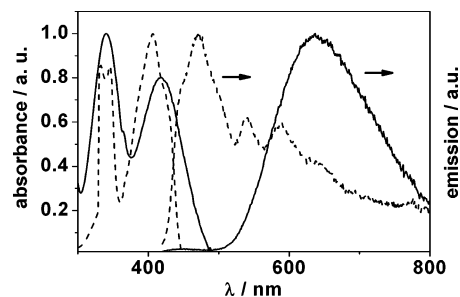


Figure 2. Normalized absorption and fluorescence spectra of 2-butylamino-6-methyl-4-nitropyridine *N*-oxide in acetonitrile (solid curves) and cyclohexane (dashed curves).

carried out under magic angle conditions to avoid the influence of the reorientational motion on the detection of the dynamics of the probe molecules.

Quantum chemical calculations were performed using two approaches. With the Gaussian 03 suite of quantum chemical programs,²⁸ we optimized the ground- and excited-state geometries at the Hartree–Fock (HF) and Configuration Interaction Singles (CIS) levels, respectively, employing the 6-311++G** basis set.^{29,30} At the optimized ground-state geometry, additional single-point energy calculations were carried out using second-order perturbation theory with Møller–Plesset (MP2) partitioning³¹ for the ground state. Density functional calculations were performed using the TURBOMOLE 5.7 suite of programs.^{32–35} The calculations used a Gaussian AO basis set of triple- ζ quality augmented with a double set of polarization functions (def-TZVP³⁶), the hybrid B3-LYP functional,^{37,38} a large grid for numerical quadrature (“grid m3” option), and convergence of the ground-state energy and density matrix to at least 10^{−8} au. The geometry of the molecule in the ground and excited states was optimized using analytical DFT and TD-DFT³⁹ gradients, respectively.

By now it has been well established that one should apply TD-DFT calculations with caution when dealing with excited states that are characterized by significant charge transfer. In particular, it has been noticed that excitation energies are usually underestimated. The validity of DFT in calculating excitation energies for similar aromatic systems was discussed by Jamorski and co-workers (see ref 40 and references therein).

For the calculations, we have considered the two isomers depicted in Figure 1. We notice that other local minima can be located on the ground- and excited-state potential energy surfaces by a rotation of about 180° around the aryl–amino bond of the amino-H isomer. However, in the ground state these conformers lack the contribution of an internal hydrogen bond and are accordingly found to be considerably higher in energy. In the subsequent part of this Article, they will therefore not be considered any further.

III. Results and Discussion

A. Steady-State Spectra and Quantum Chemical Calculations. Previous experimental UV spectra^{41,42} and quantum chemical calculations^{43–45} suggest that the lowest two excited singlet states are the charge-transfer and the ¹L_b states,⁴⁶ respectively, and that the direction of the CT is dependent on the type of substituents attached to the pyridine ring.^{47,48}

The steady-state absorption and emission spectra of the presently investigated derivative, 2B6M, are shown in Figure 2. We notice that the Stokes shift is rather solvent dependent, reaching a value of about 8000 cm^{−1} in acetonitrile. The absorption spectrum, on the other hand, shows only minor

TABLE 1: Energy Difference (kJ/mol) between the Two Tautomeric (N–O····HN and N–O–H····N) Forms of 2-Butylamino-6-methyl-4-nitropyridine N-Oxide for the Ground and First Excited States

method	basis	ground state	excited state
		$E(S_0') - E(S_0)^a$	$E(S_1') - E(S_1)^a$
HF/CIS	6-311++G**	32	-22
MP2	6-311++G**	56	
(TD-)DFT	def-TZVP	54	-9

^a Primed and unprimed labels refer to the N–O····HN and N–O–H····N species, respectively.

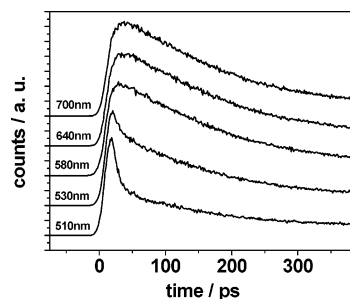
polarity dependence. The fact that the excitation spectrum (not shown here) and the absorption spectrum overlap in polar aprotic solvents corroborates the hypothesis that in these solvents only one ground-state species exists. In apolar solvents such as cyclohexane, in contrast, it is found that the excitation spectrum does not coincide with the absorption spectrum, which indicates that there are two or more coexisting ground-state species present. We suspect that dimers might be one of the other species. The observation that the shape of the absorption and fluorescence spectrum does not show any concentration dependence in polar aprotic solvents indicates, however, that in these solvents we do not have any significant contribution of dimers. The very weak signal around 450 nm in acetonitrile solution is probably due to impurities.

The results of the quantum chemical calculations are consistent with the experimentally recorded absorption and emission spectra. The isomers considered in these calculations correspond to local minima both on the ground- and on the excited-state potential energy surfaces (PESs). The relative energies of the ground- and excited-state isomers are compiled in Table 1. All methods predict that for the ground state the amino-H isomer is more stable than the other tautomer by 30–60 kJ/mol. The calculations reveal that the S_1 state is dominated by the HOMO → LUMO configuration for both isomers. This transition results in a significant charge transfer from the pyridine ring in the direction of the nitro group, as well as from the amino group (NH–Bu) to the ring. Excited-state relaxation does not alter the character of the excited state. For the S_1 state, a reversal of the stability of the two isomers occurs; now the N–O–H isomer is found to be lower in energy by 10–20 kJ/mol. To obtain insight into the vibrational effects on the relative order of the first excited state of the two isomers, the zero-point energies (ZPEs) have been calculated in the case of the ground state using the harmonic frequencies. Because the effect of the ZPEs on the calculated energy differences is about 1 kJ/mol, it is irrelevant to the current study and can be ignored.

Table 2 reports the calculated vertical absorption and emission transition energies. The performance of the CIS method is rather poor, while the DFT transition energies are in excellent agreement with the experimental results. Comparison of the calculated and experimental vertical excitation energies strongly suggests that excitation takes place from the amino-H isomer, in agreement with the calculated stabilities of the two tautomeric forms in the ground state. The calculated and experimental

TABLE 2: Calculated Transition Wavelengths (nm) for Vertical Absorption and Emission of the Two Tautomeric Forms of 2-Butylamino-6-methyl-4-nitropyridine N-Oxide

method	basis	absorption		emission	
		N–O····HN	N–O–H····N	N–O····HN	N–O–H····N
		$S_0 \rightarrow S_1^*$	$S_0' \rightarrow S_1'^*$	$S_1^* \rightarrow S_0$	$S_1'^* \rightarrow S_0'$
CIS	6-311++G**	261	288	302	357
TD-DFT	def-TZVP	428	519	511	640
exp.		417			636

**Figure 3.** Fluorescence decay curves at various wavelengths as measured in acetonitrile by time-correlated single photon counting.

fluorescence wavelengths reveal that emission occurs predominantly from the N–O–H isomer.

B. Time-Resolved Experiments. Figure 3 shows typical fluorescence transients detected at various emission wavelengths. When detecting at the blue side of the emission band, for example, 510 nm, a fast decrease followed by a slow decay is observed, while detection at longer wavelengths, for example, 580 nm, shows the appearance of a corresponding fast rise. The curves can be well fitted with a biexponential function. The long component of ~ 150 ps is independent of the probing wavelength and has a relative amplitude that is increasing toward longer detection wavelengths. This component can be well assigned to the lifetime of the equilibrated emissive state. Apart from the long component, the fits find a short component on the order of a few picoseconds. An accurate determination of this component is more difficult because of the instrument response of ~ 16 ps. Results of the fits are summarized in Table 3. As a further attempt to determine the ultrafast dynamics, femtosecond transient absorption experiments have been performed.

Femtosecond transient absorption spectra are shown in Figure 4. After excitation at 420 nm, two broad absorption bands around 400 and 650 nm emerge almost instantaneously (Figure 4a), accompanied by a bleaching around 420 nm. Subsequently, another absorption band around 530 nm appears, which rises with a time constant of ~ 0.6 ps. Simultaneously a broad stimulated emission band emerges between 650 and 800 nm that rises with the same time constant. After the initial spectral dynamics, the whole spectrum decays (Figure 4b) at a rate matching the emissive lifetime of the excited state determined in the TC-SPC experiments (~ 150 ps). This picture becomes more clear when we look at individual transients, for example, at 740 nm (insets in Figure 4). The transient at 740 nm is composed of two components: a positive absorption signal with an ultrashort decay time around 100 fs as determined by fitting the transient, and a negative, stimulated emission signal that grows in with a time constant of ~ 0.6 ps (Figure 4a), which corresponds to the response limited picosecond component in the SPC measurement (Table 3), and subsequently decays with ~ 150 ps (Figure 4b).

The presence of an absorption band centered around 650 nm with an ultrashort lifetime is at odds with the intramolecular

TABLE 3: Fits of the Fluorescence Transients of 2-Butylamino-6-methyl-4-nitropyridine *N*-Oxide Dissolved in Acetonitrile to a Biexponential Function $I(\lambda, t) = a_1(\lambda) e^{-t/\tau_1(\lambda)} + a_2(\lambda) e^{-t/\tau_2(\lambda)}$ Convolved with the Instrument Response^a

emission wavelength (nm)	τ_1 (ps)	a_1	τ_2 (ps)	a_2
510	5 ± 5	$89.1(\pm 5\%)$	149 ± 5	$10.9(\pm 10\%)$
530	7 ± 5	$66.5(\pm 6\%)$	151 ± 5	$33.5(\pm 5\%)$
580	3 ± 5	$-87.6(\pm 20\%)$	156 ± 5	$100(\pm 5\%)$
640	8 ± 5	$-19.3(\pm 19\%)$	157 ± 5	$100(\pm 5\%)$
740	6 ± 5	$-19.1(\pm 47\%)$	150 ± 5	$100(\pm 4\%)$

^a The sum of positive amplitudes is taken as 100.

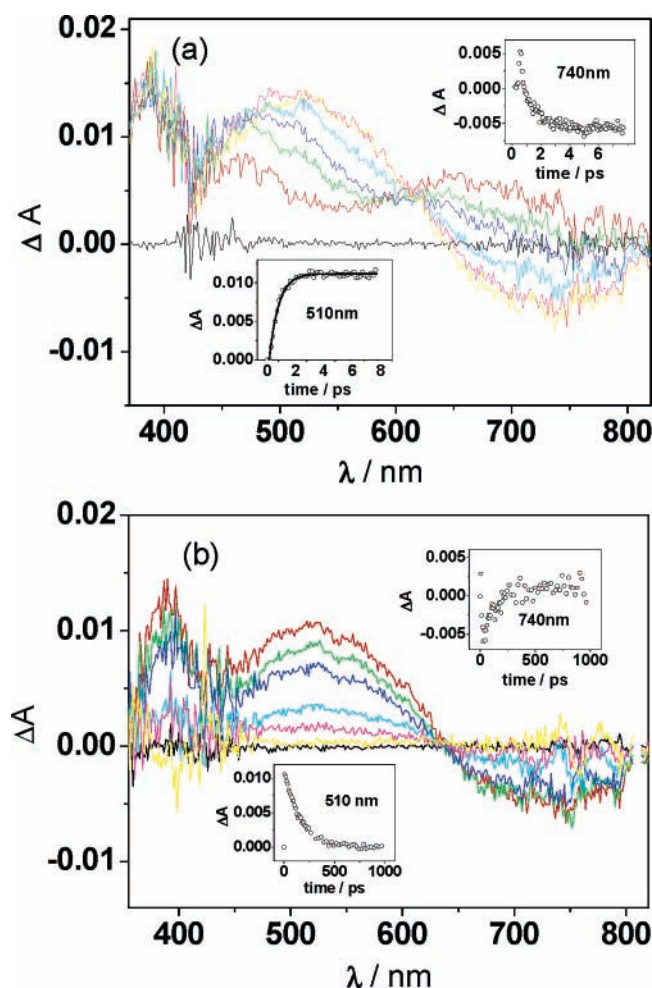


Figure 4. Transient absorption spectra of 2-amino-6-methyl-4-nitropyridine *N*-oxide in acetonitrile obtained after excitation at 420 nm. Part (a) shows spectra for short pump–probe delays: -0.3 ps (black), 0.1 ps (red), 0.2 ps (green), 0.3 ps (dark blue), 0.7 ps (light blue), 1.9 ps (magenta), 5.9 ps (yellow). Part (b) shows the spectra for longer delay times: 0 ps (black), 20 ps (red), 50 ps (green), 100 ps (dark blue), 200 ps (light blue), 300 ps (magenta), 800 ps (yellow).

charge-transfer model that has been widely accepted for the parent molecule 4-nitropyridine *N*-oxide.⁴⁹ In this model, photoexcitation is assumed to bring the molecule directly from the ground electronic state (which has a small dipole moment) to its ICT state, without population of a locally excited state. The ultrashort living absorption band around 650 nm can therefore not be assigned to a locally excited state but is associated with the ICT state before the proton transfer occurs. Our quantum chemical calculations indicate that the S_1 state of the present amino-substituted derivative has significant charge-

transfer character, giving rise to a dipole moment in the excited state that is significantly different from that of the ground state. The change in dipole moment upon excitation would result in a solvent reorganization effect when the molecule is dissolved in a polar solvent such as acetonitrile, and manifest itself in the time-resolved absorption spectrum as a dynamic Stokes shift.⁵⁰ Our experiments show, in contrast, that the initially excited species evolves on an ultrafast time scale into another species with distinctly different absorption and emission characteristics. Following the results of the quantum chemical calculations, we attribute this species to the tautomer of the molecule. In this picture, the absorption band centered around 650 nm is ascribed to excited-state absorption from the S_1 state of the amino-H isomer. Depopulation of this state by proton transfer leads to the population of the excited state of the $N-O-H$ isomer.

The present results imply a relatively large ES IPT rate that merits some further comments. In 2-amino-6-methyl-4-nitropyridine *N*-oxide, phototautomerization takes place via a pseudo five-membered ring. Such a process is generally assumed to be slower than in molecules where proton transfer occurs in a pseudo six-membered ring geometry. Although in the first instance the presently observed proton-transfer rate might therefore seem to be rather large, it is not without precedent: in 3-hydroxyflavone a similar five-membered ring proton transfer occurs on time scales of 30–60 fs.⁵¹ Our quantum chemical calculations, which find stable minima for both tautomers in the excited state, imply a barrier for proton transfer. Although we have not been able to determine this barrier by geometry optimization of the transition state, we do find a relatively large decrease of the unscaled NH stretch frequency from 3532 to 3290 cm^{-1} upon excitation. This implies a relatively strong NHO bond and is consistent with a low barrier for tautomerization in the excited state.

The time-resolved spectra show that it takes about 0.6 ps for our molecular system in acetonitrile to reach its equilibrium in the excited state. Because the reorganization of acetonitrile is known to occur on the same time scale,⁵⁰ we assign this process to the solvation dynamics of acetonitrile. The associated dynamic Stokes shift was indeed observed in the picosecond fluorescence decay measurements; that is, a fast fluorescence decay, limited by the instrument response, appears when detecting on the blue side of the emission band, and a corresponding rise is observed when detecting at the red side of the emission band. A similar shift is, however, not directly visible in the femtosecond transient absorption experiments. The apparent lack of a dynamic Stokes shift in these experiments can be ascribed to the richness of the transient absorption spectrum, which comprises the excited-state absorption, ground-state bleaching, and stimulated emission of two species. The overlap of these bands obstructs the distinct appearance of a spectral shift. For example, the stimulated emission of the $N-O-H$ isomer can only be observed between 650 and 800 nm due to the strong broad absorption band centered at 530 nm. From the picosecond fluorescence decay measurements, we have established that the dynamics observed for detection wavelengths longer than 580 nm are very similar; that is, no spectral shift is seen in this wavelength range.

We thus conclude that in a polar aprotic solvent photoexcitation of 2B6M leads to intramolecular charge redistribution and that the excited, charge-transferred molecules leave the Franck–Condon region almost exclusively via proton transfer in around 100 fs. The highly polar excited state of the proton-transferred species is subsequently subject to solvent reorganiza-

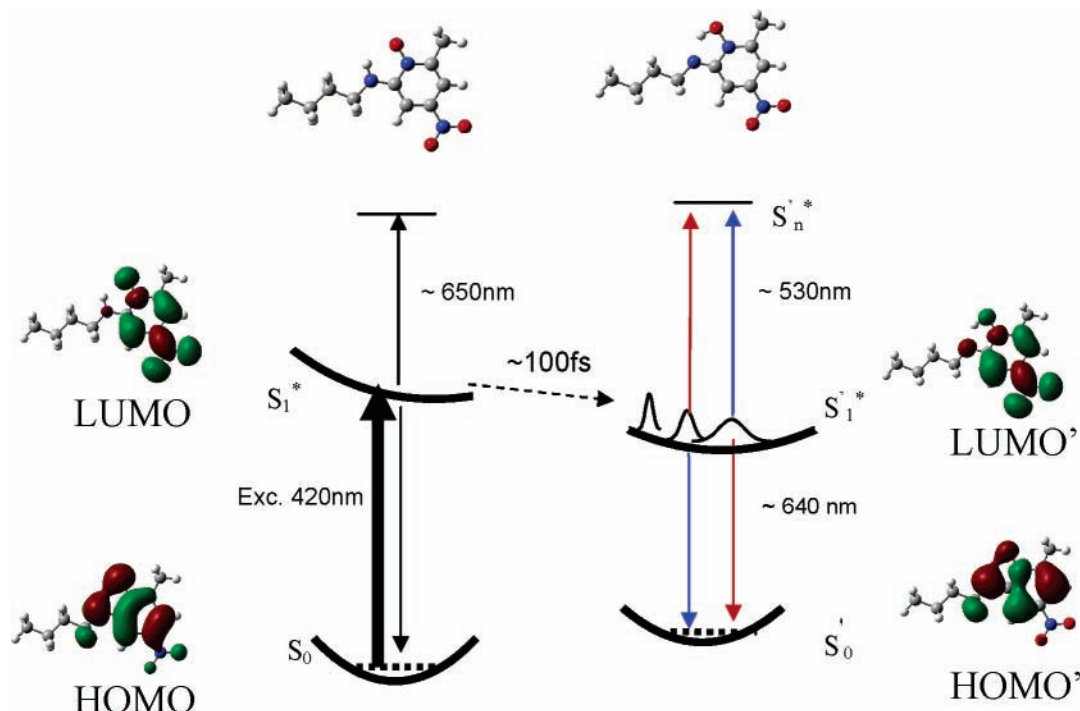


Figure 5. Scheme of the excited-state processes of 2-butylamino-6-methyl-4-nitropyridine *N*-oxide in polar aprotic solutions.

tion, prior to relaxation to the ground state. A scheme of the dynamic processes is presented in Figure 5.

A final point worth noticing is that dissipative vibrational relaxation processes are not observed in the transient absorption spectrum. After photoexcitation, molecules will experience vibrational energy relaxation to reach an equilibrium distribution, unless only the lowest vibrational levels are selectively excited, which is generally not the case in the condensed phase. During this process, excess vibrational energy is transferred to the solvent and the molecule relaxes to the lowest vibrational levels, which is detected as a shift of the emission and/or absorption band. The absence of a spectral shift on the picosecond time scale for 2B6M in acetonitrile implies that many vibrational modes are involved in the relaxation process and/or that the relaxation process is too fast to follow, similar to what is observed for Coumarin 153. For the latter molecule, vibrational excitation relaxation out of the higher energy modes was shown to be ultrafast (~ 30 fs), and the effect of subsequent dissipative relaxation of the thermalized vibrational energy on the time-resolved (subpicosecond) fluorescence spectra negligible.⁵⁰

IV. Conclusions

The present study by femtosecond transient absorption and picosecond time-resolved emission experiments, as well as quantum chemical calculations, has elucidated the electronic and structural dynamic processes occurring after excitation of 2-butylamino-6-methyl-4-nitropyridine *N*-oxide in polar, aprotic solvents. In such solvents, it has been concluded that the molecule is exclusively in one conformation. We have shown that upon excitation an intramolecular charge redistribution occurs that triggers proton transfer. This proton-transfer process takes place on a time scale around 100 fs. It is concluded that the dynamic Stokes shift occurs in the proton-transfer tautomer, which is in stark contrast to the situation in the parent molecule, 4-nitropyridine *N*-oxide, where internal charge transfer is the cause.

Acknowledgment. We would like to thank to Michiel Groeneveld for technical assistance and Dr. Paolo Proposito (Università degli Studi di Roma) for stimulating discussions and help with our steady-state and SPC experiments. This work has been supported by the Marie Curie Training Network MolPhotonics (HPMT-CT-2001-00311) and by the Hungarian Scientific Research Fund (Contract Nos. D-48583 and T-42546).

References and Notes

- (1) Youssif, S. *ARKIVOC* **2001**, 242.
- (2) Albini, A.; Pietra, S. *Heterocyclic N-Oxide*; CRC Press: Boca Raton, FL, 1991.
- (3) Lipiński, J. *J. Quantum Chem.* **1988**, *2*, 197.
- (4) Berdys, J.; Makowski, M.; Makowska, M.; Puszko, A.; Chmurzynski, L. *J. Phys. Chem.* **2003**, *107*, 6293.
- (5) Kaczmarczyk, E.; Puszko, A.; Lorenc, J.; Chmurzynski, L. *Molecules* **1999**, *4*, 94.
- (6) Zyss, J.; Chemia, D. S.; Nicoud, J. F. *J. Chem. Phys.* **1981**, *74*, 4800.
- (7) Oudar, J. L.; Chemia, D. S. *J. Chem. Phys.* **1977**, *66*, 2664.
- (8) Oudar, J. L. *J. Chem. Phys.* **1977**, *67*, 446.
- (9) Lagalante, A. F.; Jacobson, R. J.; Bruno, T. *J. Org. Chem.* **1996**, *61*, 6404.
- (10) Chmurzynski, L. *Molecules* **1997**, *2*, 169.
- (11) Agmon, N. *J. Phys. Chem. A* **2005**, *109*, 13.
- (12) Joshi, H.; Kamounah, F. S.; Gooijer, C.; van der Zwan, G.; Antonov, L. *J. Photochem. Photobiol., A* **2002**, *152*, 183.
- (13) Douhal, A.; Sanz, M.; Carranza, M. A.; Organero, J. A.; Santos, L. *Chem. Phys. Lett.* **2004**, *394*, 54.
- (14) Chou, P. T.; Pu, S. C.; Cheng, Y. M.; Yu, W. S.; Yu, Y. C.; Hung, F. T.; Hu, W. P. *J. Phys. Chem. A* **2005**, *109*, 3777.
- (15) Waluk, J. *Conformational Analysis of Molecules in Excited States*; Wiley-VCH: New York, 2000; pp 57–98.
- (16) Elsaesser, T. *Femtosecond Chem.* **1995**, *2*, 563.
- (17) Nibbering, E. T. J.; Elsaesser, T. *Chem. Rev.* **2004**, *104*, 1887.
- (18) Weiss, J.; May, V.; Ernsting, N. P.; Farzidinov, V.; Muhlfordt, A. *Chem. Phys. Lett.* **2001**, *346*, 503.
- (19) Lochbrunner, S.; Stock, K.; Riedle, E. *J. Mol. Struct.* **2004**, *700*, 13.
- (20) Lochbrunner, S.; Wurzer, A. J.; Riedle, E. *J. Chem. Phys.* **2000**, *112*, 10699.
- (21) Zhang, H.; van der Meulen, P.; Glasbeek, M. *Chem. Phys. Lett.* **1996**, *153*, 97.
- (22) Wang, H.; Zhang, H.; Abou-Zied, O. K.; Yu, C.; Romesberg, F. E.; Glasbeek, M. *Chem. Phys. Lett.* **2002**, *367*, 599.

- (23) Ameer-Beg, S.; Ormson, S. M.; Poteau, X.; Brown, R. G.; Foggi, P.; Bussotti, L.; Neuwahl, F. V. R. *J. Phys. Chem. A* **2004**, *108*, 6938.
- (24) Takeuchi, S.; Tahara, T. *J. Phys. Chem. A* **2005**, *109*, 10199.
- (25) Mitra, S.; Tamai, N.; Mukherjee, S. *J. Photochem. Photobiol., A* **2006**, *178*, 76.
- (26) Proposito, P.; Marks, D.; Zhang, H.; Glasbeek, M. *J. Phys. Chem. A* **1998**, *102*, 8894.
- (27) Balkowski, G.; Szemik-Hojniak, A.; van Stokkum, I. H. M.; Zhang, H.; Buma, W. J. *J. Phys. Chem. A* **2005**, *109*, 3535.
- (28) Frisch, M. J.; Trucks, G. W.; Schlegel, H. B.; Scuseria, G. E.; Robb, M. A.; Cheeseman, J. R.; Montgomery, J. A., Jr.; Vreven, T.; Kudin, K. N.; Burant, J. C.; Millam, J. M.; Iyengar, S. S.; Tomasi, J.; Barone, V.; Mennucci, B.; Cossi, M.; Scalmani, G.; Rega, N.; Petersson, G. A.; Nakatsuji, H.; Hada, M.; Ehara, M.; Toyota, K.; Fukuda, R.; Hasegawa, J.; Ishida, M.; Nakajima, T.; Honda, Y.; Kitao, O.; Nakai, H.; Klene, M.; Li, X.; Knox, J. E.; Hratchian, H. P.; Cross, J. B.; Adamo, C.; Jaramillo, J.; Gomperts, R.; Stratmann, R. E.; Yazyev, O.; Austin, A. J.; Cammi, R.; Pomelli, C.; Ochterski, J. W.; Ayala, P. Y.; Morokuma, K.; Voth, G. A.; Salvador, P.; Dannenberg, J. J.; Zakrzewski, V. G.; Dapprich, S.; Daniels, A. D.; Strain, M. C.; Farkas, Ö.; Malick, D. K.; Rabuck, A. D.; Raghavachari, K.; Foresman, J. B.; Ortiz, J. V.; Cui, Q.; Baboul, A. G.; Clifford, S.; Cioslowski, J.; Stefanov, B. B.; Liu, G.; Liashenko, A.; Piskorz, P.; Kom'aromi, I.; Martin, R. L.; Fox, D. J.; Keith, T.; Al-Laham, M. A.; Peng, C. Y.; Nanayakkara, A.; Challacombe, M.; Gill, P. M. W.; Johnson, B.; Chen, W.; Wong, M. W.; Gonzalez, C.; Pople, J. A. *Gaussian 03*, revision B.01; Gaussian, Inc.: Pittsburgh, PA, 2003.
- (29) Hariharan, P. C.; Pople, J. A. *Theor. Chim. Acta* **1973**, *28*, 213.
- (30) Krishnan, R.; Binkley, J. S.; Seeger, R.; Pople, J. A. *J. Chem. Phys.* **1980**, *72*, 650.
- (31) Möller, C.; Plesset, M. S. *Phys. Rev.* **1934**, *46*, 618.
- (32) Treutler, O.; Ahlrichs, R. *J. Chem. Phys.* **1995**, *102*, 346.
- (33) Arnim, M. V.; Ahlrichs, R. *J. Comput. Chem.* **1998**, *19*, 1746.
- (34) Deglmann, P.; Furche, F.; Ahlrichs, R. *Chem. Phys. Lett.* **2002**, *362*, 511.
- (35) Deglmann, P.; Furche, F. *J. Chem. Phys.* **2002**, *117*, 9535.
- (36) Schäfer, A.; Huber, C.; Ahlrichs, R. *J. Chem. Phys.* **1994**, *100*, 5829.
- (37) Lee, C.; Yang, W.; Parr, R. G. *Phys. Rev. B* **1988**, *37*, 785.
- (38) Becke, D. J. *J. Chem. Phys.* **1993**, *98*, 5648.
- (39) Furche, F.; Ahlrichs, R. *J. Chem. Phys.* **2002**, *117*, 7433.
- (40) Jamorski, C.; Foresman, J. B.; Thilgen, C.; Lüthi, H. P. *J. Chem. Phys.* **2002**, *116*, 8761.
- (41) Chmurzyński, L.; Pawlak, Z.; Myszka, H. *J. Mol. Struct.* **1982**, *80*, 235.
- (42) Wawrzynów, A.; Sokołowski, K.; Chmurzyński, L.; Liwo, A. *J. Mol. Struct.* **1988**, *174*, 235.
- (43) Kulkarni, G. V.; Ray, A.; Patel, C. C. *J. Mol. Struct.* **1981**, *71*, 253.
- (44) Lane, P.; Murray, J. S. *J. Mol. Struct.* **1991**, *236*, 283.
- (45) Puzsko, A. *J. Mol. Struct.* **1995**, *344*, 1.
- (46) Szemik-Hojniak, A.; Głowiak, T.; Puzsko, A.; Talik, Z. *J. Mol. Struct.* **1998**, *449*, 77.
- (47) Myazaki, H.; Kubota, T. *Bull. Chem. Soc. Jpn.* **1972**, *45*, 78.
- (48) Yamakawa, M.; Kubota, T.; Ezumi, K.; Mizuno, Y. *Spectrochim. Acta* **1974**, *30*, 2103.
- (49) Pierre, M.; Baldeck, P. L.; Block, D.; Georges, R.; Trommsdorff, H. P. *Chem. Phys.* **1991**, *156*, 103.
- (50) Horng, M. L.; Gardecki, J. A.; Papazyan, A.; Maroncelli, M. *J. Phys. Chem.* **1995**, *99*, 17311.
- (51) Ameer-Beg, S.; Ormson, S. M.; Brown, R. G.; Matousek, P.; Towrie, M.; Nibbering, E. T. J.; Foggi, P.; Neuwahl, F. V. R. *J. Phys. Chem. A* **2001**, *105*, 3709.